

1 **Biomining of Cu₂S nanoparticles by *Geobacter sulfurreducens***

2 Richard L. Kimber,^a# Heath Bagshaw,^{a1} Kurt Smith,^{a2} Dawn M. Buchanan,^a Victoria S. Coker,^a

3 Jennifer S. Cavet,^b Jonathan R. Lloyd^a

4 ^aWilliamson Research Centre for Molecular Environmental Science, Department of Earth

5 and Environmental Sciences, University of Manchester, Manchester, UK

6 ^bSchool of Biological Sciences, Faculty of Biology Medicine and Health, University of

7 Manchester, Manchester, UK

8

9 Running Head: Biomining of Cu₂S nanoparticles

10 Keywords: *Geobacter sulfurreducens*; copper, nanoparticles, Cu₂S, bioreduction

11 #Address correspondence to Richard L. Kimber, richard.kimber@manchester.ac.uk

12

13

14

15

16

¹ Imaging Centre at Liverpool, University of Liverpool, Liverpool L69 3GL, UK

² Chemical Sciences Division, Lawrence Berkeley National Laboratory, Berkeley, CA, 94720, USA

17 Abstract

18 Biomineralization of Cu has been shown to control contaminant dynamics and transport in
19 soils. However, very little is known about the role that subsurface microorganisms may play
20 in the biogeochemical cycling of Cu. In this study, we investigate the bioreduction of Cu(II)
21 by the subsurface metal-reducing bacterium, *Geobacter sulfurreducens*. Rapid removal of Cu
22 from solution was observed in cell suspensions of *G. sulfurreducens* when supplied with
23 Cu(II), while transmission electron microscopy (TEM) analyses showed the formation of
24 electron dense nanoparticles associated with the cell surface. Energy-dispersive X-ray
25 spectroscopy (EDX) point analysis and EDX spectrum image maps revealed the nanoparticles
26 are rich in both Cu and S. This was confirmed by x-ray absorption near edge structure
27 (XANES) and extended X-Ray absorption fine structure (EXAFS) analyses which identified the
28 nanoparticles as Cu₂S. Biomineralization of Cu_xS nanoparticles in soils has been reported to
29 enhance the colloidal transport of a number of contaminants including Pb, Cd, and Hg.
30 However, formation of these Cu_xS nanoparticles has only been observed under sulfate-
31 reducing conditions and could not be repeated using isolates of implicated organisms. As *G.*
32 *sulfurreducens* is unable to respire sulfate, and no reducible sulfur was supplied to the cells,
33 these data suggest a novel mechanism for the biomineralization of Cu₂S under anoxic
34 conditions. The implications of these findings for the biogeochemical cycling of Cu and other
35 metals as well as the green production of Cu catalysts are discussed.

36 Importance

37 Dissimilatory metal-reducing bacteria are ubiquitous in soils and aquifers and are known to
38 utilize a wide range of metals as terminal electron acceptors. These transformations play an

39 important role in the biogeochemical cycling of metals in pristine and contaminated
40 environments and can be harnessed for bioremediation and metal bioprocessing purposes.
41 However, relatively little is known about their interactions with Cu. As a trace element that
42 becomes toxic in excess, Cu can adversely affect soil biota and fertility. In addition,
43 biomineralization of Cu nanoparticles has been reported to enhance mobilization of other
44 toxic metals. Here, we demonstrate that when supplied with acetate under anoxic
45 conditions, the model metal-reducing bacterium, *Geobacter sulfurreducens*, can transform
46 soluble Cu(II) to Cu₂S nanoparticles. This study provides new insights into Cu
47 biomineralization by microorganisms and suggests that contaminant mobilization enhanced
48 by Cu biomineralization could be facilitated by *Geobacter* species and related organisms.

49

50 Introduction

51 Dissimilatory metal-reducing bacteria are ubiquitous in soils and aquifers and are able to
52 respire a wide range of metals coupled to the oxidation of organic or inorganic compounds
53 (1, 2). These processes play an important role in the biogeochemical cycling of metals in
54 soils and subsurface environments (3, 4). In addition, microbial metal reduction can be
55 harnessed for catalytic applications (5, 6) and bioremediation purposes (7, 8). Species of
56 *Geobacter* and *Shewanella* are among the most intensively studied metal reducers due to
57 their presence in many soil and freshwater environments, respiratory diversity and
58 availability of genomic data (9-11). These organisms are able to utilise a range of metals as
59 terminal electron acceptors including Fe(III), Mn(IV), U(VI), Pu(VI), Cr(VI), Ag(I), Pd(II), and
60 V(V) (3, 12-18). These processes typically involve c-type cytochromes, which facilitate
61 electron transfer from the inner membrane to the periplasm and outer membrane, where

62 many of these metals are reduced (19-21). Although the versatility of these metal-reducers
63 is well established, relatively little is known about their interactions with Cu.

64 Cu is a widely encountered trace element with its distribution in soil affected by climate,
65 geology and soil properties (22). In addition, anthropogenic sources can lead to elevated Cu
66 concentrations (23-26). Cu is an essential trace metal found in almost all forms of life,
67 however, it can also be highly toxic by binding to proteins and inactivating enzyme function
68 or by catalysing Fenton chemistry to produce reactive oxygen species. Thus at elevated
69 concentrations, the inherent toxicity of Cu can limit plant growth, lowering crop yield and
70 quality (27-29), and decrease microbial community diversity and activity (30). Microbial
71 processes play an important role in controlling the environmental fate of metals, potentially
72 immobilizing them via redox changes including bioreduction or through sulfidation reactions
73 (31). However, biomineralization has also been reported to enhance the mobilization of Cu
74 and other co-contaminants through the formation of colloidal Cu nanoparticles (25, 32). For
75 example, Hofacker *et al.* suggested *Clostridium* sp. were responsible for the Cu nanoparticle
76 formation under soil reducing conditions, however, they were unable to directly observe
77 Cu(II) reduction in cell suspensions of the *Clostridium* isolates (33). Therefore further work is
78 required to identify subsurface microorganisms which can potentially influence the
79 biogeochemical behaviour of this important micronutrient.

80

81 We demonstrated recently that *S. oneidensis* is able to reductively precipitate Cu(0)
82 nanoparticles from a Cu(II)-containing solution (6). Interestingly, the use of deletion mutants
83 revealed that *c*-type cytochromes in the Mtr-pathway, commonly used to reduce metals in
84 *Shewanella* species, did not play a role in Cu(II) reduction. The as-prepared Cu-

85 nanoparticles were shown to be catalytically active towards a range of 'click-chemistry'
86 cycloaddition reactions, which have applications in the pharmaceutical industry (34).
87 Here we investigate the fate of Cu(II) when supplied to cultures of another well
88 characterised model metal-reducing bacterium, the obligate anaerobe *G. sulfurreducens*, in
89 order to better understand its potential role in the biogeochemical cycling and fate of Cu in
90 contaminated soils and sediments, including the ability to produce Cu nanoparticles. Cu
91 toxicity towards *G. sulfurreducens* was examined and its ability to bioreduce Cu(II) and
92 remove the metal from solution monitored using inductively coupled plasma atomic
93 emission spectroscopy (ICP-AES). Any biomineralization products were analysed using
94 transmission electron microscopy (TEM), scanning transmission electron microscopy
95 (STEM), energy-dispersive X-ray spectroscopy (EDX), X-ray absorption near edge structure
96 (XANES), and extended X-Ray absorption fine structure (EXAFS).

97

98 Results

99 Cu(II) toxicity towards *G. sulfurreducens*

100 The effect of a range of concentrations of Cu on the anaerobic growth of *G. sulfurreducens*
101 in minimal medium with lactate and fumarate supplied as the electron donor and acceptor
102 respectively, is shown in Figure 1. Supplementation of the medium with 100 nM and 1 μ M
103 Cu(II) had little or no effect on the growth of *G. sulfurreducens* relative to a control with no
104 added Cu(II). However, supplementation with 10 μ M Cu(II), caused an extended lag phase
105 with little to no growth seen over the initial 24 hours and only 45 % growth seen after 48
106 hours relative to the no added Cu(II) control. With 100 μ M Cu(II) supplementation, no

107 growth was observed after 48 hours. Hence, under anoxic conditions growth of *G.*

108 *sulfurreducens* is strongly inhibited by Cu at 10 μ M and above.

109

110 Removal of Cu(II) and formation of Cu nanoparticles

111 Based on data from the toxicity assay, and guided by Cu pore-water concentrations in
112 contaminated soils (25, 35), Cu(II) concentrations of 5 and 50 μ M were chosen to be used in
113 resting cell experiments to investigate potential bioreduction of Cu(II) and possible
114 formation of lower oxidation state Cu nanoparticles, noted recently in cultures of other
115 metal-reducing bacteria (6). Initial Cu(II) concentrations were confirmed via sampling of the
116 solution prior to the addition of cells (t_0). A decrease in the soluble Cu solution
117 concentrations of 30.3 % and 12.0 % was observed in control experiments performed with
118 dead (autoclaved) cells with initial concentrations of 5 μ M and 50 μ M Cu(II), respectively
119 (Figure 2). This decrease was observed at the first time point, taken immediately after
120 inoculating the Cu(II)-containing medium with cells (t_1), and then remained constant,
121 consistent with initial Cu removal via rapid passive sorption to the biomass. In the presence
122 of live cells and electron donor (acetate), a substantial further increase in Cu removal from
123 solution compared to the dead (autoclaved) cell controls was observed, suggesting that the
124 majority of Cu removal in these treatments was facilitated by metabolic processes, rather
125 than by passive biosorption to the cell biomass (Figure 2). When supplied with 5 μ M Cu(II),
126 50 % Cu removal was observed immediately after adding the cells (t_1) which then increased
127 to 80% removal at 1 hour. Cu removal remained stable at ~80% at 24 hours, with a small
128 decrease to 73% seen at the final 72 hour time point. When supplied with an initial
129 concentration of 50 μ M Cu(II), only 36% of the Cu was removed by the live cells at the first

130 time point (t1). Removal of Cu continued slowly for up to 24 hours, reaching a maximum of
131 63% removal at 24 hours before decreasing again slightly to 58% removal at 72 hours.
132 Oxygenated cell controls (with acetate) showed decreased Cu removal at all time points
133 compared to the anoxic cells when challenged with either 5 μ M or 50 μ M Cu(II). When no
134 electron donor was supplied, initial Cu removal was slightly enhanced relative to the
135 acetate-amended system when challenged with 5 μ M Cu(II). However, after 3 hours, Cu
136 solution concentrations remained relatively stable in the acetate-amended experiment but
137 a significant increase in Cu solution concentrations was observed in both the electron donor
138 free and oxygenated cell controls. When the final time point was taken at 72 hours, Cu
139 removal was greatest in the anoxic cells supplied with acetate for both the 5 μ M and 50 μ M
140 Cu(II) challenged systems.

141

142 TEM images of samples taken at 24 hours demonstrated that when supplied with acetate as
143 an electron donor under anoxic conditions, removal of Cu by *G. sulfurreducens* resulted in
144 the biomineralisation of Cu nanoparticles (Figure 3). These Cu nanoparticles were typically
145 spherical and predominately associated with the cells, ranging in size from 10 to 90 nm.

146 EDX point analysis indicated that the particles were both Cu and S rich (Figure 3). This was
147 further supported by EDX spectrum imaging performed during STEM that revealed a close
148 association between Cu and S in the nanoparticles (Figure 4). A small number of particles
149 were also seen in the dead (autoclaved) control, however these were typically larger (100 -
150 200 nm) agglomerates and were far fewer than with live cells supplied with acetate. EDX
151 analysis indicated these particles were also Cu and S rich (Figure S1, Supporting

Information). No nanoparticles were observed in the oxygenated cells control or no electron donor control (Figure S2, Supporting Information).

X-ray absorption spectroscopy (XAS) characterization

To identify the speciation of Cu and the local valence structure of the metallic nanoparticles, XAS characterisation was performed on B18 at the Diamond Light Source. The Cu K-edge X-ray absorption near edge structure (XANES) spectrum collected on the Cu nanoparticles precipitated by *G. sulfurreducens* had an absorption edge energy (E_0) of 8980.4 eV. This aligned well with the E_0 energy of a Cu_2S (chalcocite) standard (8980.1 eV). The excellent match between the XANES spectra for the Cu nanoparticles and the Cu_2S standard clearly demonstrates that washed cell suspensions of the metal-reducing bacterium *G. sulfurreducens* catalysed the formation of Cu_2S particles (Figure 5a). The oxidation state of Cu in Cu_2S is thought to be dominated by Cu(I), however, the presence of significant Cu(II) and Cu(0) has also been suggested (36, 37). XANES data were identical whether the Cu nanoparticles were formed when the cells were supplied with Cu(II) as CuSO_4 or CuCl_2 , ruling out any impact from the salt (data not shown).

Given the similarity between the Cu nanoparticles and Cu_2S XANES spectra, the Cu nanoparticle EXAFS data were fitted assuming a similar coordination environment as the mineral chalcocite (Cu_2S) (38). The best fit (Figure 5b) was obtained with one shell of 3 S atoms at 2.30 ± 0.01 Å with a Debye-Waller factor of 0.009 ± 0.001 . This is consistent with a Cu_2S -like structure where Cu is coordinated by 3 S atoms at approximately 2.3 Å. Cu_2S has 6 Cu atoms in the second shell, however, the Cu-S interatomic distance is poorly constrained (2.60 - 3.30 Å), and which is likely to reduce the contribution from Cu scatterers to the

EXAFS spectrum. Given this, the EXAFS data do not preclude the formation of a Cu₂S phase. See Table S1 (Supporting Information) for complete description of the EXAFS fitting. Collectively, the XANES and EXAFS data support the biomineralization of the Cu(II) as poorly ordered Cu₂S.

Cu L_{2,3}-edge XAS was also performed on selected samples at the Advanced Light Source, Berkeley. When live cells were supplied with an electron donor, peaks at 930.7 and 933.4 eV were observed (Figure S3, Supporting Information). The peak at 930.7 eV is indicative of Cu(II) whereas the peak at 933.4 eV reflects the presence of Cu(I) (39, 40). Although the peak at 930.7 eV is qualitatively larger than the peak at 933.4 eV, the Cu(II) is known to be approximately 25 times more intense than the Cu(I) peak (39), suggesting a significant presence of Cu(I) in the sample, confirming bioreduction took place. Cu L_{2,3}-edge XAS data from the autoclaved and no electron donor controls also display peaks indicative of Cu(II) and Cu(I), although with a noticeable shift of +0.3 eV in peak positions. The intensity of the Cu(I) peaks are qualitatively smaller in both controls compared to the live cells supplied with electron donor, suggesting less Cu bioreduction occurred in the controls.

190

191 Discussion

192 Cu toxicity towards *G. sulfurreducens*

Our results demonstrate that under anoxic conditions, concentrations as low as 10 µM Cu(II) strongly inhibit the growth of *G. sulfurreducens*. This is over an order of magnitude lower than the Cu(II) concentrations (>100 µM) that are reported to be required to inhibit the growth of the enteric model organism *Escherichia coli* under similar conditions (anoxic

197 chemically defined media) (39). In a recent study, the model Fe(III)-reducing bacterium
198 *Shewanella oneidensis*, also appears to have greater resistance to Cu toxicity than *G.*
199 *sulfurreducens* with some growth of *S. oneidensis* still observed at 100 μ M Cu in a similar
200 chemically defined medium (6, 40), whereas growth of *G. sulfurreducens* is inhibited
201 completely (Figure 1). Hence, *G. sulfurreducens* appears to be particularly vulnerable to Cu
202 toxicity.

203 Bio mineralization of Cu nanoparticles

204 The relatively low tolerance of *G. sulfurreducens* towards Cu(II) compared to *S. oneidensis* is
205 also reflected in their respective ability to reduce Cu(II). In our previous study, complete
206 reduction of 50 μ M and partial reduction of up to 200 μ M Cu(II) to Cu(0) was observed by *S.*
207 *oneidensis* (6). In the present study, *G. sulfurreducens* was only capable of removing up to 80
208 % and 63 % of 5 μ M and 50 μ M Cu(II) from solution, respectively. No removal at 200 μ M
209 Cu(II) was observed (data not shown). Our data suggest that Cu removal from solution is
210 greatest in the presence of live cells, suggesting that microbial metabolism increases
211 removal of Cu from solution compared to biosorption by dead biomass. The highest removal
212 was seen when live cells were supplied with an electron donor under anoxic conditions, with
213 TEM and XAS data indicating that formation of Cu nanoparticles was significant only under
214 these conditions. This suggests that the presence of an electron donor and anoxic conditions
215 are required for significant biosynthesis of Cu nanoparticles. Characterisation of these
216 nanoparticles as Cu₂S is supported by EDX point analysis, EDX mapping, XANES and EXAFS
217 data. As no nanoparticles were seen in the oxygenated or electron donor free controls and
218 XAS data support limited reduction to Cu(I) species, we attribute the observed removal of
219 Cu from solution under these conditions to biosorption of Cu(II) to the cell surface and/or

220 intracellular accumulation of the metal. Interestingly, the Cu solution concentrations in the
221 oxygenated and electron donor free controls were found to increase after 3 hours, but
222 remained relatively stable under anoxic conditions with an electron donor (acetate). We
223 suggest that the rerelease of Cu into solution observed in the oxygenated and electron
224 donor free controls may be due to export of intracellular Cu and/or desorption of cell-bound
225 Cu, which was limited in the anoxic cells supplied with acetate due to immobilization of Cu
226 via bioreduction and Cu₂S precipitation.

227 The formation of Cu₂S nanoparticles here is surprising as previous work on Cu
228 biomineralization by anaerobic bacteria found that, in the absence of sulfate-reducing
229 conditions, nanoparticles formed were metallic Cu or Cu oxides (6, 25, 41, 42). A number of
230 mechanisms have been proposed for the formation of Cu(0) nanoparticles among different
231 bacteria. Ramanathan *et al.* suggested that intracellular reduction and cellular efflux
232 systems may play a role in the synthesis of extracellular Cu(0) nanoparticles by *M. morganii*
233 (42). *Clostridium* species were implicated in the formation of Cu(0) nanoparticles in a
234 flooded Cu contaminated soil via cellular efflux of Cu(I) followed by disproportionation to
235 Cu(II) and Cu(0) (25, 33). Conversion of the Cu(0) nanoparticles to Cu_xS in the flooded soil
236 was observed following the onset of sulfate reduction. As *G. sulfurreducens* is unable to
237 carry out dissimilatory sulfate reduction, this cannot account for the of Cu₂S nanoparticles
238 seen here. Identical XANES spectra from Cu nanoparticles formed when *G. sulfurreducens*
239 were supplied with Cu(II) as CuSO₄ and CuCl₂ further supports a mechanism which does not
240 directly involve sulfate reduction. Clearly, a different mechanism is responsible for the
241 biomineralization of Cu₂S nanoparticles in *G. sulfurreducens* compared to the Cu(0)
242 nanoparticles typically produced by other bacteria studied to date.

243 Cell bound thiol sites have been shown to dominate metal(oid) complexation in a range of
244 microorganisms, including *G. sulfurreducens* (43, 44). In addition, intracellular Cu(I) is known
245 to target Fe-S clusters in *E. coli* under anoxic conditions with Cu(I) displacing the Fe (45-47).
246 Ligation of Cu with these sulfur groups could potentially play a role in the formation of Cu_xS
247 nanoparticles in organisms which are unable to reduce Cu(II) to Cu(0), such as *G.*
248 *sulfurreducens*. However, elucidating the mechanisms of Cu nanoparticle formation in
249 metal-reducing bacteria requires further work and will be the target of future studies.

250 This study demonstrates that *G. sulfurreducens*, a metal-reducing bacteria, is able to
251 produce Cu₂S nanoparticles from aqueous Cu(II). This provides direct evidence of Cu
252 biomineralization by a ubiquitous subsurface microorganism which may suggest a role for
253 this organism in the biogeochemical cycling of Cu and potential mobilization of co-
254 contaminants in soil systems (25). Cu_xS nanoparticles have previously been reported to form
255 only following the onset of sulfate reduction. *G. sulfurreducens* is unable to respire sulfate,
256 suggesting that biomineralisation of Cu_xS nanoparticles could also occur in the absence of
257 sulfate-reducing conditions. In addition to the biogeochemical implications discussed above,
258 biomineralization of Cu nanoparticles offers a promising green method for the production of
259 Cu catalysts. We have previously demonstrated that Cu(0) nanoparticles produced by *S.*
260 *oneidensis* are active click chemistry catalysts (6). Cu₂S nanoparticles also have a number of
261 catalytic applications, including as electrocatalysts for oxygen evolution and CO₂ reduction
262 (48, 49). Therefore, tailored Cu nanoparticle catalysts could potentially be produced using
263 specific microorganisms.

264

265 **Materials and Methods**

266 *Geobacter sulfurreducens*

267 All cultures of *G. sulfurreducens* (ATCC 51573) were grown anaerobically in a fully defined,
268 pre-sterilized, liquid minimal medium (NBAF) (50) at pH 7.1. Serum bottles (100 ml)
269 containing NBAF were inoculated with a late log/early stationary phase culture to give an
270 optical density of 0.02 at 600 nm. The cultures were grown for 24 hours at 30 °C. Late log
271 cultures were transferred under anoxic conditions to centrifuge tubes, and the cells pelleted
272 by centrifugation at 4,960 rpm for 20 minutes at 4 °C. The cells were washed two times with
273 fresh anoxic, sterilised MOPS buffer (50 mM) and then were resuspended in the same buffer
274 at pH 7.1.

275 Toxicity assay

276 Cells were grown in minimal media as described above. Late-log phase aliquots were used
277 to inoculate 50 ml of anoxic minimal media to give a starting optical density of 0.015. Cu
278 (CuSO₄) was added from a stock solution to give a final concentration of 0.1, 1, 10, 100 or
279 µM Cu(II). A Cu free control was also used. Incubation was carried out at 30°C. Samples
280 were taken under anoxic, aseptic conditions at 0, 4, 8, 24, and 48 hours and the optical
281 density measured to determine growth. All conditions were performed in triplicate with a
282 standard deviation of less than 0.012 between OD₆₀₀ readings.

283 Cu removal experiments

284 The removal of Cu(II) by *G. sulfurreducens* was determined using pre-grown and washed
285 “resting cell” cultures supplied with excess electron donor. The cultures contained either 5
286 µM or 50 µM Cu(II) as CuSO₄ (unless stated otherwise) and 30 mM sodium acetate as the
287 electron donor in 50 mM MOPS adjusted to pH 7.1. The medium was purged with a gas mix

288 of N₂:CO₂ (80:20) for 20 minutes to remove O₂, sealed with thick butyl rubber stoppers and
289 autoclaved. Washed late log/early stationary phase cells were then added aseptically to
290 achieve a final optical density of 0.2 and incubation was carried out at 30 °C. Soluble Cu was
291 determined by taking aliquots centrifuging at 14,900 g for 10 minutes to pellet the cells and
292 insoluble Cu. Samples were taken from the supernatant and Cu in solution measured using
293 ICP-AES. All experiments were performed in triplicate.

294 TEM imaging

295 All sample preparations were performed under anoxic conditions in an anaerobic cabinet. 1
296 ml of cell suspension from the Cu reduction assay (5 and 50 µM) was taken after 24 hours
297 and centrifuged at 14900 g for 10 minutes, the supernatant discarded and the pellet
298 resuspended in 1 ml deionised water. 1.5 µl of the cell suspension was pipetted onto a gold
299 TEM grid with a carbon-coated formvar or holey-carbon support film and air dried in an
300 anaerobic chamber. Samples were kept anoxic until they were transferred into the TEM
301 chamber. TEM imaging and EDX analysis were performed in an FEI TF 30 FEG Analytical TEM
302 operated at 300kV and equipped with an Oxford X-max80 Windowless SSD EDS system. EDX
303 analysis was performed with the sample tilted at the optimum angle towards the detector
304 to increase collection efficiency.

305 STEM

306 STEM imaging and EDX analysis were performed in a FEI Talos F200A AEM with anX-FEG
307 electron source operated at 200 kV. High angle annular dark field (HAADF) STEM imaging
308 was performed using a probe current of approximately 250 pA. EDX analysis was performed

309 using a Super-X four silicon drift EDX detector system with a total collection solid angle of
310 0.7 sr, all four detectors were turned on and the sample was not tilted.

311 X-ray absorption spectroscopy (XAS) characterization

312 For XAS characterisation at the Cu K-edge, 1 ml aliquots of the *G. sulfurreducens* Cu
313 reduction (5 and 50 μM of CuSO_4 and CuCl_2) assays were taken and centrifuged at 14900 g
314 for 10 minutes. The supernatant was discarded and the pellet resuspended in 1 ml anoxic
315 deionised water. The sample was centrifuged again, resuspended in 1 ml anoxic deionised
316 water before 200 μl of the suspension was pipetted onto a plastic weighing boat and air
317 dried. Samples were mounted onto a layer of kapton tape which in turn was mounted onto
318 an aluminium sample holder. A further layer of kapton tape was applied over the samples to
319 maintain anaerobicity. X-ray absorption fine structure (XAFS) spectra were collected at the
320 Cu K-edge (~ 8980 eV) at room temperature on beamline B18 at the Diamond Light Source. A
321 36-element solid-state Ge detector with digital signal processing for fluorescence XAFS, high
322 energy resolution, and high count rate was used to measure with the beam at 45° incidence
323 with respect to the sample holder plane. All spectra were acquired in quick-EXAFS mode,
324 using the Pt-coated branch of collimating and focusing mirrors, a Si(111) double-crystal
325 monochromator and a pair of harmonic rejection mirrors.

326 XAS processing and background subtraction was carried out using Athena whereas EXAFS
327 data were modelled using Artemis (Demeter(51); 0.9.24). Fitting was calculated using
328 multiple k-weights (k , k^2 , and k^3) and the best fit was calculated in R space by minimisation
329 of the reduced χ^2 . At no point did the parameterisation utilise more than $\frac{2}{3}$ of the
330 independent points available.

331 Cu L_{2,3}-edge spectroscopy was performed at the Advanced Light Source, Berkeley, USA on
332 beamline 6.3.1.1. For sample preparation 1 ml aliquots were taken and centrifuged at
333 14900 g for 10 minutes. The supernatant was discarded and the pellet resuspended in 1 ml
334 anoxic deionised water. The sample was centrifuged again before final resuspension in 1 ml
335 anoxic deionised water. 200 µl of the suspension was dried as a powder onto a carbon sticky
336 pad before being placed on an aluminium sample holder and stored under anoxic conditions
337 prior to analysis. All manipulations were performed in an anaerobic chamber. X-ray
338 absorption spectra were collected in total-electron yield (TEY) mode and normalised to the
339 incident beam intensity.

340

341 Acknowledgments

342 The authors would like to thank NERC for funding under the Resource Recovery from Waste
343 program (NE/L014203/1), and also acknowledges support from the BBSRC (grants
344 BB/L013711/1 and BB/R010412/1). The authors would also like to P. Lythgoe (University of
345 Manchester) for ICP-AES analysis. K.S. would like to acknowledge EnvRadNet and
346 ST/K001787/1 for funding. The authors acknowledge beamtime awarded at the Diamond
347 Light Source for XANES and EXAFS on beamline B18 under proposals SP-13705 and SP-
348 16136. We would like to thank Giannantonio Cibirri for his assistance on B18. This research
349 used resources of the Advanced Light Source, a DOE Office of Science User Facility under
350 contract no. DE-AC02-05CH11231

351

352 References

- 353 1. Lovley DR, Phillips EJP. 1988. Novel mode of microbial energy metabolism: organic carbon
354 oxidation coupled to dissimilatory reduction of iron or manganese. *Appl Environ Microbiol*
355 **54**:1472.
- 356 2. Lovley DR. 1993. Dissimilatory metal reduction. *Annu Rev Microbiol* **47**:263-90.
- 357 3. Lovley DR, Holmes DE, Nevin KP. 2004. Dissimilatory Fe(III) and Mn(IV) reduction. *Adv*
358 *Microb Physiol* **49**:219-86.
- 359 4. Williamson AJ, Morris K, Shaw S, Byrne JM, Boothman C, Lloyd JR. 2013. Microbial reduction
360 of Fe(III) under alkaline conditions relevant to geological disposal. *Appl Environ Microbiol*
361 **79**:3320.
- 362 5. Søbberg LS, Gauthier D, Lindhardt AT, Bunge M, Finster K, Meyer RL, Skrydstrup T. 2009. Bio-
363 supported palladium nanoparticles as a catalyst for Suzuki–Miyaura and Mizoroki–Heck
364 reactions. *Green Chem* **11**:2041-6.
- 365 6. Kimber RL, Lewis EA, Parmeggiani F, Smith K, Bagshaw H, Starborg T, Joshi N, Figueroa AI,
366 van der Laan G, Cibir G, Gianolio D, Haigh SJ, Pattrick RAD, Turner NJ, Lloyd JR. 2018.
367 Biosynthesis and characterization of copper nanoparticles using *Shewanella oneidensis*:
368 application for click chemistry. *Small* **14**:1703145.
- 369 7. Lloyd JR. 2003. Microbial reduction of metals and radionuclides. *FEMS Microbiol Rev* **27**:411-
370 25.
- 371 8. Gadd GM. 2010. Metals, minerals and microbes: geomicrobiology and bioremediation.
372 *Microbiology* **156**:609-43.
- 373 9. Methé BA, Nelson KE, Eisen JA, Paulsen IT, Nelson W, Heidelberg JF, Wu D, Wu M, Ward N,
374 Beanan MJ, Dodson RJ, Madupu R, Brinkac LM, Daugherty SC, DeBoy RT, Durkin AS, Gwinn
375 M, Kolonay JF, Sullivan SA, Haft DH, Selengut J, Davidsen TM, Zafar N, White O, Tran B,
376 Romero C, Forberger HA, Weidman J, Khouri H, Feldblyum TV, Utterback TR, Van Aken SE,
377 Lovley DR, Fraser CM. 2003. Genome of *Geobacter sulfurreducens*: metal reduction in
378 subsurface environments. *Science* **302**:1967.

- 379 10. Heidelberg JF, Paulsen IT, Nelson KE, Gaidos EJ, Nelson WC, Read TD, Eisen JA, Seshadri R,
380 Ward N, Methe B, Clayton RA, Meyer T, Tsapin A, Scott J, Beanan M, Brinkac L, Daugherty S,
381 DeBoy RT, Dodson RJ, Durkin AS, Haft DH, Kolonay JF, Madupu R, Peterson JD, Umayam LA,
382 White O, Wolf AM, Vamathevan J, Weidman J, Impraim M, Lee K, Berry K, Lee C, Mueller J,
383 Khouri H, Gill J, Utterback TR, McDonald LA, Feldblyum TV, Smith HO, Venter C, Nealson KH,
384 Fraser CM. 2002. Genome sequence of the dissimilatory metal ion-reducing bacterium
385 *Shewanella oneidensis*. *Nat Biotechnol* **20**:1118.
- 386 11. Fredrickson JK, Romine MF. 2005. Genome-assisted analysis of dissimilatory metal-reducing
387 bacteria. *Curr Opin Biotechnol* **16**:269-74.
- 388 12. Marshall MJ, Beliaev AS, Dohnalkova AC, Kennedy DW, Shi L, Wang Z, Boyanov MI, Lai B,
389 Kemner KM, McLean JS, Reed SB, Culley DE, Bailey VL, Simonson CJ, Saffarini DA, Romine
390 MF, Zachara JM, Fredrickson JK. 2006. c-Type cytochrome-dependent formation of U(IV)
391 nanoparticles by *Shewanella oneidensis*. *PLoS Biol* **4**:e268.
- 392 13. Icopini GA, Lack JG, Hersman LE, Neu MP, Boukhalfa H. 2009. Plutonium(V/VI) reduction by
393 the metal-reducing bacteria *Geobacter metallireducens* GS-15 and *Shewanella oneidensis*
394 MR-1. *Appl Environ Microbiol* **75**:3641.
- 395 14. Liu C, Gorby YA, Zachara JM, Fredrickson JK, Brown CF. 2002. Reduction kinetics of Fe(III),
396 Co(III), U(VI), Cr(VI), and Tc(VII) in cultures of dissimilatory metal-reducing bacteria.
397 *Biotechnol Bioeng* **80**:637-49.
- 398 15. Belchik SM, Kennedy DW, Dohnalkova AC, Wang Y, Sevinc PC, Wu H, Lin Y, Lu HP,
399 Fredrickson JK, Shi L. 2011. Extracellular reduction of hexavalent chromium by Cytochromes
400 MtrC and OmcA of *Shewanella oneidensis* MR-1. *Appl Environ Microbiol* **77**:4035-41.
- 401 16. Law N, Ansari S, Livens FR, Renshaw JC, Lloyd JR. 2008. Formation of nanoscale elemental
402 silver particles via enzymatic reduction by *Geobacter sulfurreducens*. *Appl Environ Microbiol*
403 **74**:7090.

- 404 17. Ng CK, Cai Tan TK, Song H, Cao B. 2013. Reductive formation of palladium nanoparticles by
405 *Shewanella oneidensis*: role of outer membrane cytochromes and hydrogenases. *RSC Adv*
406 **3**:22498-503.
- 407 18. Carpentier W, Sandra K, De Smet I, Brigé A, De Smet L, Van Beeumen J. 2003. Microbial
408 reduction and precipitation of vanadium by *Shewanella oneidensis*. *Appl Environ Microbiol*
409 **69**:3636.
- 410 19. Shi L, Squier TC, Zachara JM, Fredrickson JK. 2007. Respiration of metal (hydr)oxides by
411 *Shewanella* and *Geobacter*: a key role for multiheme c-type cytochromes. *Mol Microbiol*
412 **65**:12-20.
- 413 20. Ueki T, DiDonato LN, Lovley DR. 2017. Toward establishing minimum requirements for
414 extracellular electron transfer in *Geobacter sulfurreducens*. *FEMS Microbiol Lett* **364**.
- 415 21. Levar CE, Hoffman CL, Dunshee AJ, Toner BM, Bond DR. 2017. Redox potential as a master
416 variable controlling pathways of metal reduction by *Geobacter sulfurreducens*. *The ISME*
417 *Journal* **11**:741-52.
- 418 22. Ballabio C, Panagos P, Lugato E, Huang J-H, Orgiazzi A, Jones A, Fernandez-Ugalde O, Borrelli
419 P, Montanarella L. 2018. Copper distribution in European topsoils: an assessment based on
420 LUCAS soil survey. *Sci Total Environ* **636**:282-98.
- 421 23. Pietrzak U, McPhail DC. 2004. Copper accumulation, distribution and fractionation in
422 vineyard soils of Victoria, Australia. *Geoderma* **122**:151-66.
- 423 24. Turpeinen R, Kairesalo T, Häggblom MM. 2004. Microbial community structure and activity
424 in arsenic-, chromium- and copper-contaminated soils. *FEMS Microbiol Ecol* **47**:39-50.
- 425 25. Weber F-A, Voegelin A, Kaegi R, Kretzschmar R. 2009. Contaminant mobilization by metallic
426 copper and metal sulphide colloids in flooded soil. *Nat Geosci* **2**:267-71.
- 427 26. Balasoïu CF, Zagury GJ, Deschênes L. 2001. Partitioning and speciation of chromium, copper,
428 and arsenic in CCA-contaminated soils: influence of soil composition. *Sci Total Environ*
429 **280**:239-55.

- 430 27. Mocquot B, Vangronsveld J, Clijsters H, Mench M. 1996. Copper toxicity in young maize (*Zea*
431 *mays* L.) plants: effects on growth, mineral and chlorophyll contents, and enzyme activities.
432 *Plant and Soil* **182**:287-300.
- 433 28. Maksymiec W. 1998. Effect of copper on cellular processes in higher plants. *Photosynthetica*
434 **34**:321-42.
- 435 29. Yruela I. 2005. Copper in plants. *Braz J Plant Physiol* **17**:145-56.
- 436 30. Smit E, Leeftang P, Wernars K. 1997. Detection of shifts in microbial community structure
437 and diversity in soil caused by copper contamination using amplified ribosomal DNA
438 restriction analysis. *FEMS Microbiol Ecol* **23**:249-61.
- 439 31. Anderson RT, Vrionis HA, Ortiz-Bernad I, Resch CT, Long PE, Dayvault R, Karp K, Marutzky S,
440 Metzler DR, Peacock A, White DC, Lowe M, Lovley DR. 2003. Stimulating the in situ activity of
441 *Geobacter* species to remove uranium from the groundwater of a uranium-contaminated
442 aquifer. *Appl Environ Microbiol* **69**:5884-91.
- 443 32. Hofacker AF, Voegelin A, Kaegi R, Kretzschmar R. 2013. Mercury mobilization in a flooded
444 soil by incorporation into metallic copper and metal sulfide nanoparticles. *Environ Sci*
445 *Technol* **47**:7739-46.
- 446 33. Hofacker AF, Behrens S, Voegelin A, Kaegi R, Lösekann-Behrens T, Kappler A, Kretzschmar R.
447 2015. *Clostridium* species as metallic copper-forming bacteria in soil under reducing
448 conditions. *Geomicrobiol J* **32**:130-9.
- 449 34. Kolb HC, Sharpless KB. 2003. The Growing Impact of Click Chemistry on Drug Discovery. *Drug*
450 *Discov Today* **8**:1128-37.
- 451 35. Vulkan R, Zhao F-j, Barbosa-Jefferson V, Preston S, Paton GI, Tipping E, McGrath SP. 2000.
452 Copper speciation and impacts on bacterial biosensors in the pore water of copper-
453 contaminated soils. *Environ Sci Technol* **34**:5115-21.

- 454 36. Gupta S, Chandna N, Singh AK, Jain N. 2018. Regioselective synthesis of N²-alkylated-1,2,3
455 triazoles and N¹-alkylated benzotriazoles: Cu₂S as a recyclable nanocatalyst for oxidative
456 amination of N,N-dimethylbenzylamines. *J Org Chem* **83**:3226-35.
- 457 37. Kumar P, Nagarajan R, Sarangi R. 2013. Quantitative X-ray absorption and emission
458 spectroscopies: electronic structure elucidation of Cu₂S and CuS. *J Mater Chem C* **1**:2448-54.
- 459 38. Evans Jun HT. 1971. Crystal structure of low chalcocite. *Nature Physical Science* **232**:69.
- 460 39. Outten FW, Huffman DL, Hale JA, O'Halloran TV. 2001. The independent cue and cus systems
461 confer copper tolerance during aerobic and anaerobic growth in *Escherichia coli*. *J Biol Chem*
462 **276**:30670-7.
- 463 40. Toes ACM, Geelhoed JS, Kuenen JG, Muyzer G. 2008. Characterization of heavy metal
464 resistance of metal-reducing *Shewanella* isolates from marine sediments. *Geomicrobiol J*
465 **25**:304-14.
- 466 41. Singh AV, Patil R, Anand A, Milani P, Gade W. 2010. Biological synthesis of copper oxide nano
467 particles using *Escherichia coli*. *Current Nanoscience* **6**:365-9.
- 468 42. Ramanathan R, Field MR, O'Mullane AP, Smooker PM, Bhargava SK, Bansal V. 2013. Aqueous
469 phase synthesis of copper nanoparticles: a link between heavy metal resistance and
470 nanoparticle synthesis ability in bacterial systems. *Nanoscale* **5**:2300-6.
- 471 43. Mishra B, Shoenfelt E, Yu Q, Yee N, Fein JB, Myneni SCB. 2017. Stoichiometry of mercury-
472 thiol complexes on bacterial cell envelopes. *Chem Geol* **464**:137-46.
- 473 44. Mishra B, Boyanov M, Bunker BA, Kelly SD, Kemner KM, Fein JB. 2010. High- and low-affinity
474 binding sites for Cd on the bacterial cell walls of *Bacillus subtilis* and *Shewanella oneidensis*.
475 *Geochim Cosmochim Acta* **74**:4219-33.
- 476 45. Macomber L, Imlay JA. 2009. The iron-sulfur clusters of dehydratases are primary
477 intracellular targets of copper toxicity. *PNAS* **106**:8344-9.

- 478 46. Tan G, Yang J, Li T, Zhao J, Sun S, Li X, Lin C, Li J, Zhou H, Lyu J, Ding H. 2017. Anaerobic
479 copper toxicity and iron-sulfur cluster biogenesis in *Escherichia coli*. *Appl Environ Microbiol*
480 **83**.
- 481 47. Tan G, Cheng Z, Pang Y, Landry AP, Li J, Lu J, Ding H. 2014. Copper binding in IscA inhibits
482 iron-sulphur cluster assembly in *Escherichia coli*. *Mol Microbiol* **93**:629-44.
- 483 48. Coughlan C, Ibáñez M, Dobrozhan O, Singh A, Cabot A, Ryan KM. 2017. Compound copper
484 chalcogenide nanocrystals. *Chem Rev* **117**:5865-6109.
- 485 49. An L, Zhou P, Yin J, Liu H, Chen F, Liu H, Du Y, Xi P. 2015. Phase transformation fabrication of
486 a Cu₂S nanoplate as an efficient catalyst for water oxidation with glycine. *Inorg Chem*
487 **54**:3281-9.
- 488 50. Muhamadali H, Xu Y, Ellis DI, Allwood JW, Rattray NJW, Correa E, Alrabiah H, Lloyd JR,
489 Goodacre R. 2015. Metabolic profiling of *Geobacter sulfurreducens* during industrial
490 bioprocess scale-up. *Appl Environ Microbiol* **81**:3288-98.
- 491 51. Ravel B, Newville M. 2005. ATHENA and ARTEMIS: interactive graphical data analysis using
492 IFEFFIT. *Phys Scr* **2005**:1007.
- 493
- 494
- 495
- 496
- 497
- 498
- 499
- 500

501 **Figure 1** Anaerobic growth of *G. sulfurreducens* in minimal medium (NBAF) supplemented with different Cu(II)
502 concentrations. Each concentration was performed in triplicate with error bars representing the standard
503 deviation of the replicates.

504

505 **Figure 2** Concentration of Cu in solution in the presence of *G. sulfurreducens* when supplied with an initial
506 Cu(II) concentration of (a) 5 μM and (b) 50 μM . In both cases, Cu(II) was added to the media prior to cell
507 addition. The initial concentration of Cu was confirmed via ICP-AES. The first time point (t_1) was then taken
508 immediately after cell addition. Cu in solution was calculated as the concentration of Cu at a given time point
509 (C) divided by the initial concentration prior to cell addition (C_0) as determined by ICP-AES. Experiments were
510 performed under anoxic conditions except where indicated with the addition of O_2 (purple diamonds). The
511 addition or omission of acetate as electron donor is indicated by $+\text{e}^-$ or $-\text{e}^-$, respectively. Each experiment was
512 performed in triplicate with errors representing the standard deviation of these replicates.

513

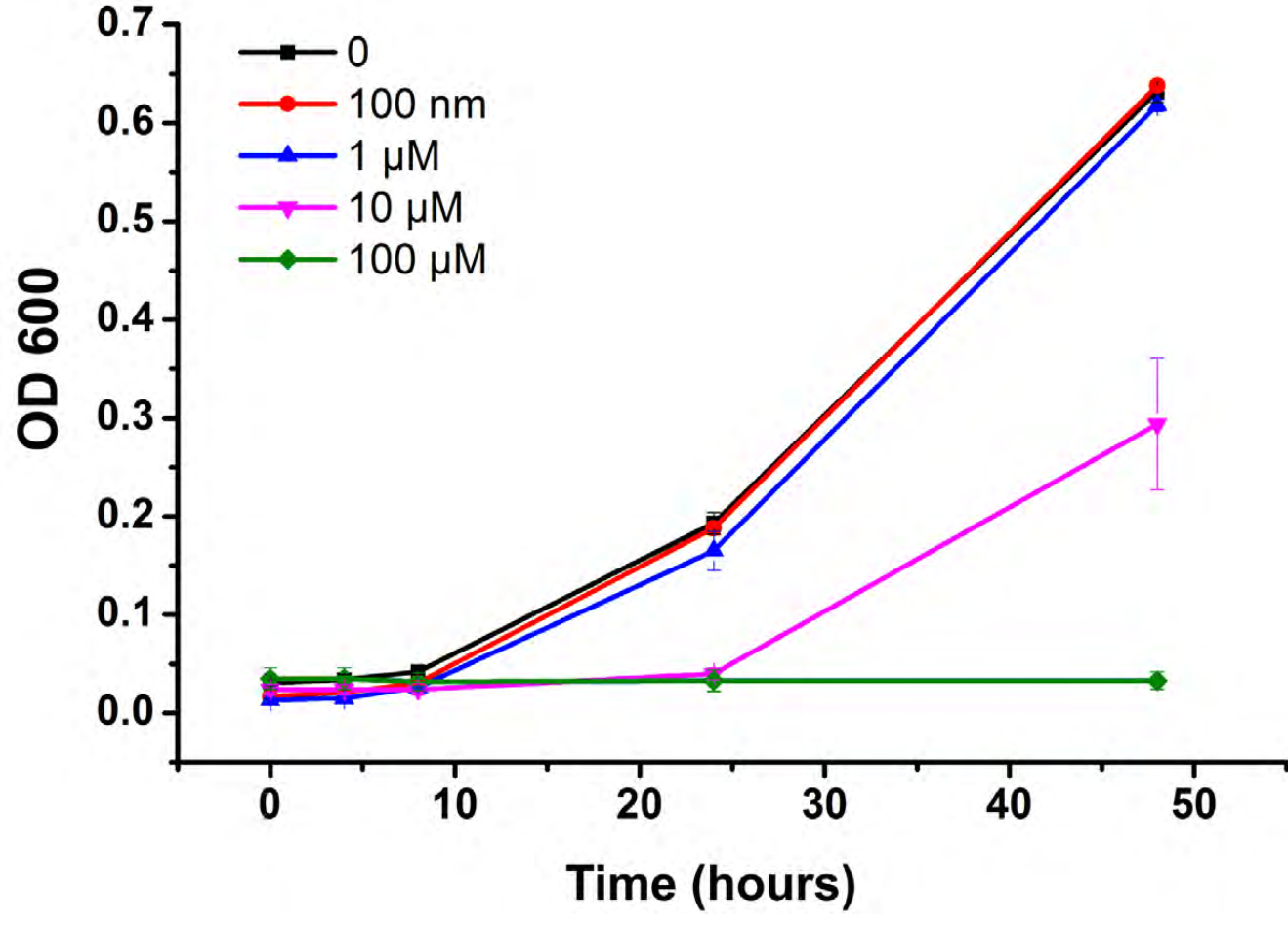
514 **Figure 3** TEM images of *G. sulfurreducens* with associated Cu nanoparticles after being supplied with (a-c) 5 μM
515 Cu(II) and (d-f) 50 μM Cu(II). The bottom row shows the corresponding EDX spectra of particles from panel a, c,
516 and e (left to right). The x axis displays energy (keV) with the y axis displaying total counts. Samples for TEM
517 imaging were taken at 24 hours.

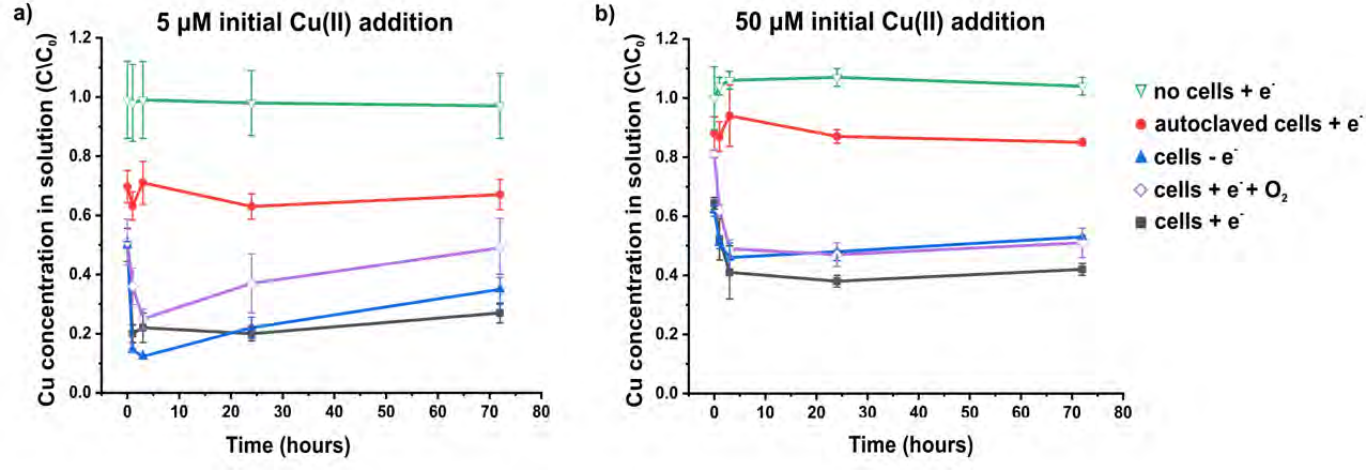
518

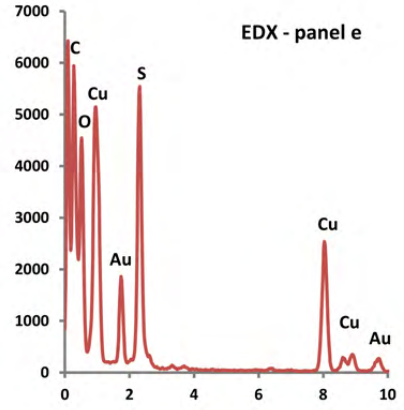
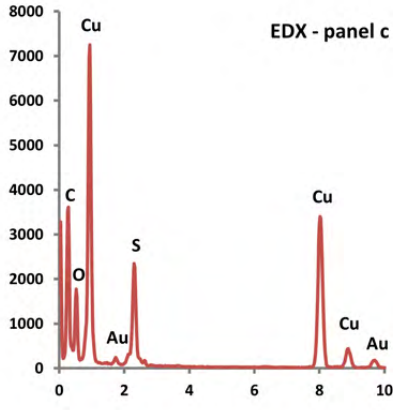
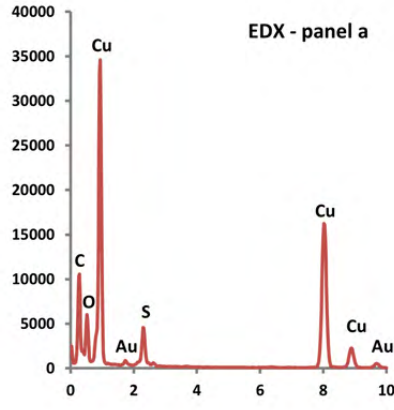
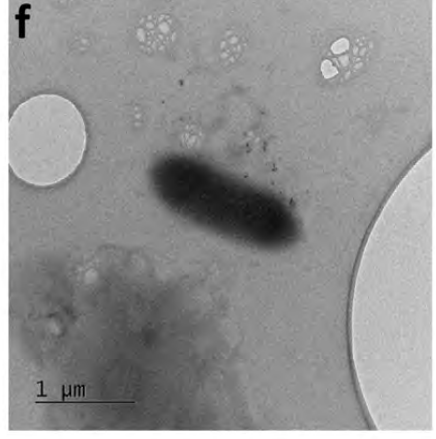
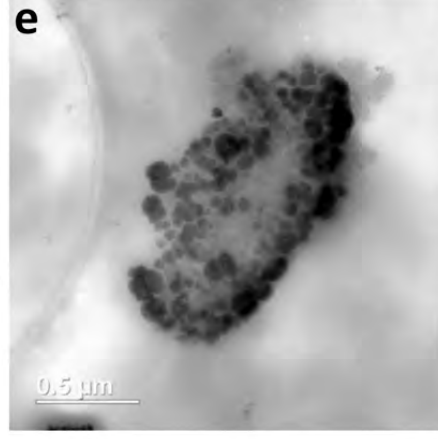
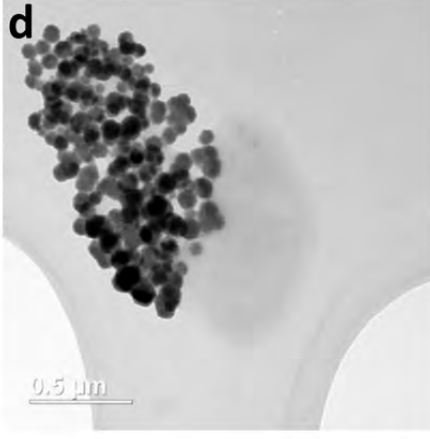
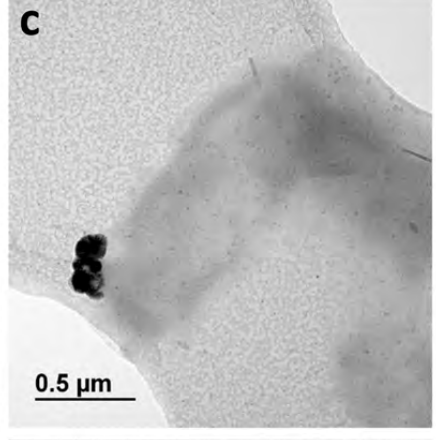
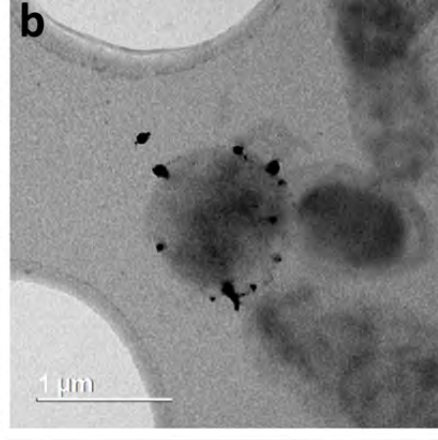
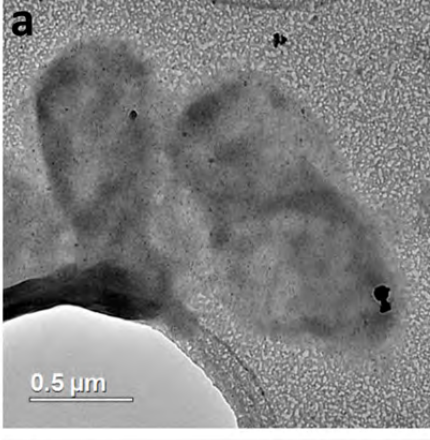
519 **Figure 4** (a) TEM image of cells with Cu nanoparticles (b) High-angle annular dark field (HAADF) image of the
520 red dashed square from (a). EDX spectrum imaging of (b) taken under STEM showing (c) Cu and (d) S.

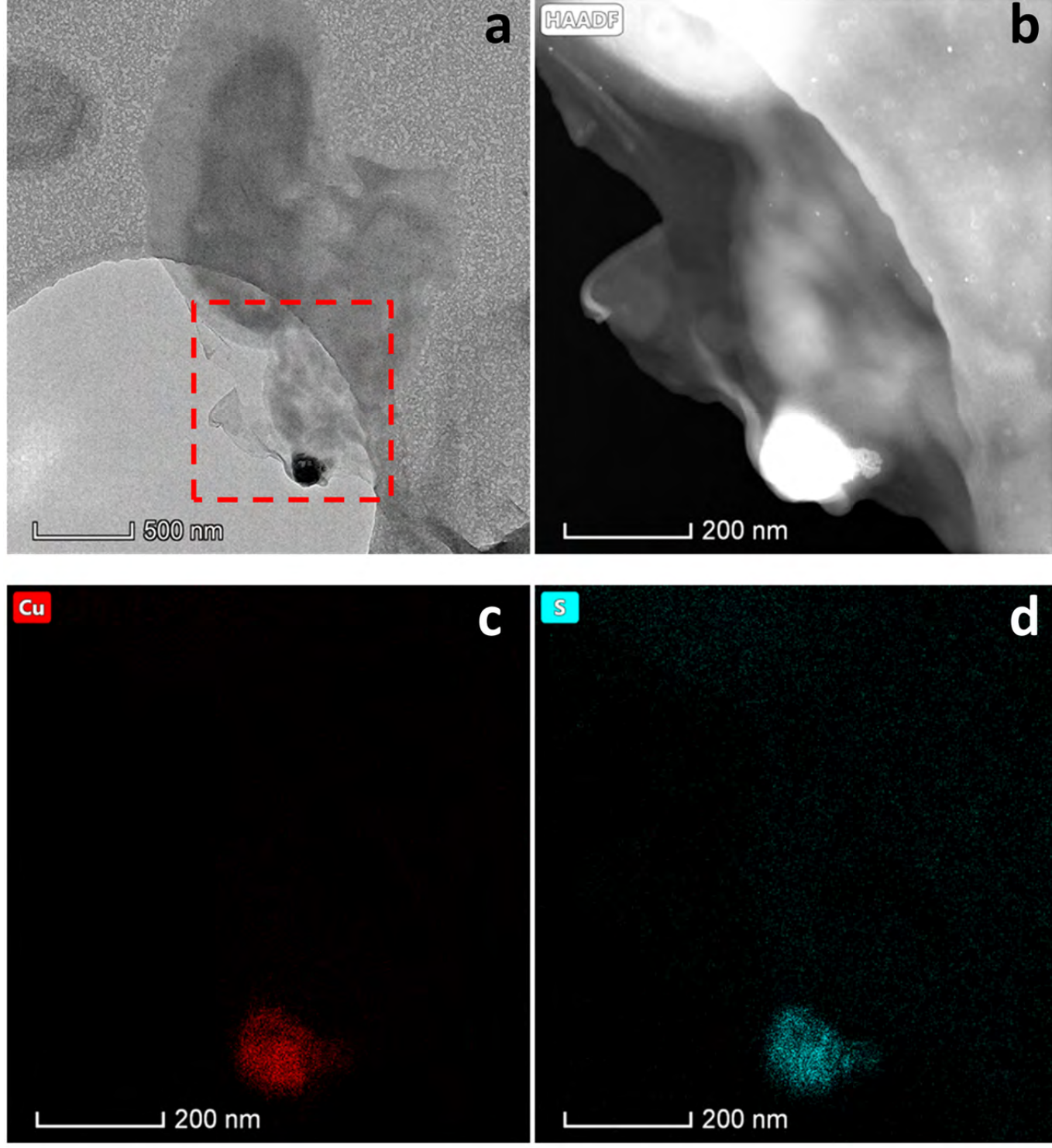
521

522 **Figure 5** (a) XANES for the Cu K-edge of Cu nanoparticles produced by *G. sulfurreducens* (black line) and Cu
523 standards. b) K^3 weighted EXAFS data and c) corresponding Fourier transform for the Cu K-edge of the Cu
524 nanoparticles (Cu-NPs). Data are shown by the black (solid) line and the fit is shown by the red (dotted) line.

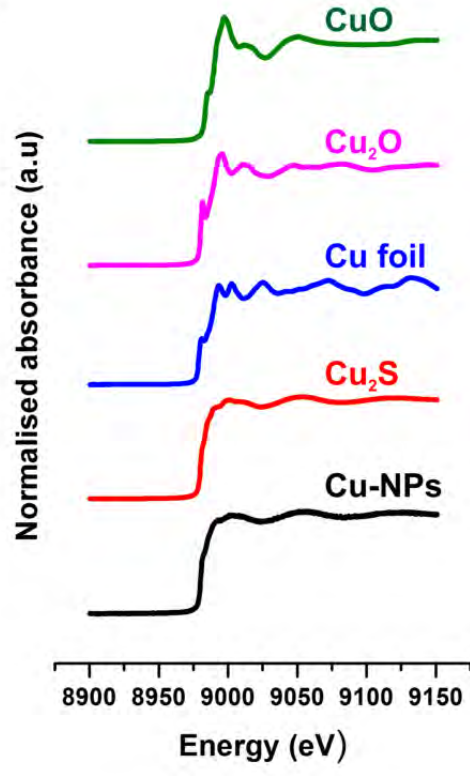




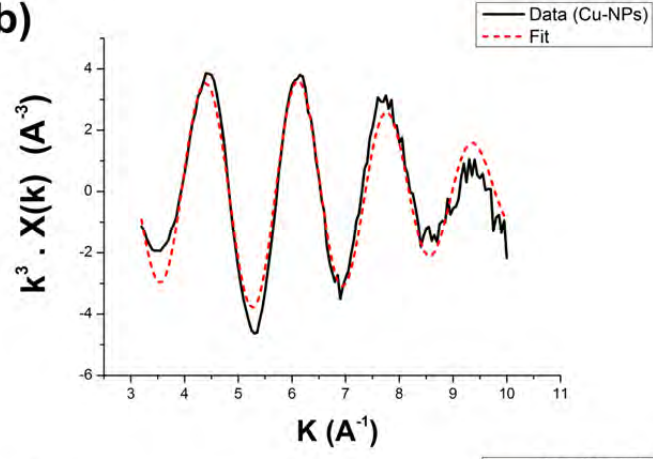




a)



b)



c)

